Simulation Studies of Field-Reversed Configurations with Rotating Magnetic Field Current Drive

E. V. Belova 1), R. C. Davidson 1),
1) Princeton University Plasma Physics Laboratory, Princeton NJ, USA

E-mail:ebelova@pppl.gov

Abstract. First results of 3D kinetic simulations of rotating magnetic field (RMF) current drive in field-reversed configuration (FRC) are presented. Self-consistent hybrid simulations have been performed using the HYM code for even- and odd-parity RMF and different FRC parameters. Simulations show that the RMF pushes the plasma radially inward, resulting in a reduced plasma density outside separatrix. Lower initial plasma density and larger RMF amplitudes result in faster RMF field penetration, in agreement with previous two-fluid studies. Numerical study of the effects of the applied RMF field on particle confinement shows that the rate of particle losses increases in larger FRCs, and with larger RMF amplitudes. High-frequency, fully-penetrated RMF can reduce ion losses provided that the RMF is of even-parity. The improved particle confinement is related to ponderomotive forces due to the rapidly oscillating, inhomogeneous electromagnetic field. In contrast, fully-penetrated odd-parity RMFs force particles away from the midplane toward the FRC ends. Partially-penetrated RMF show little difference between even and odd-parity in terms of the ion confinement.

1. Introduction

New method of formation and current drive in field-reversed configurations (FRCs) using rotating magnetic field (RMF) current drive has been successfully demonstrated in several FRC experiments. High plasma temperature and order-of-magnitude increases in the configuration life-time have been achieved. However, numerical simulations of the RMF current drive so far have been limited to 2D two-fluid simulations. This paper presents first numerical results of three-dimensional kinetic simulations of RMF-FRCs. Self-consistent hybrid simulations have been performed for even- and odd-parity RMF and different FRC parameters using nonlinear hybrid and MHD simulation code HYM [1,2]. Simulations show that the RMF pushes the plasma radially inward, resulting in a reduced plasma density outside separatrix. Lower initial plasma density and larger RMF amplitudes result in faster RMF field penetration, in agreement with previous two-fluid studies [3]. Numerical study of the effects of the applied high-frequency RMF field on particle confinement demonstrated for the first time significant and unexpected difference between RMF configurations of even- and odd-parity. It is found that high-frequency fully-penetrated RMF can reduce ion losses provided that the RMF is of even-parity. The improved particle confinement is related to ponderomotive forces due to the rapidly oscillating, inhomogeneous electromagnetic field. In contrast, odd-parity RMF forces particles away from the midplane toward the FRC ends, potentially destroying the configuration.

2. Ion Confinement

An application of even-parity RMF to FRC results in open magnetic field lines for any RMF amplitude, provided the RMF is fully penetrated, which has been a major concern

regarding the RMF current drive method. An odd-parity RMF configuration has been proposed in order to prevent field-line opening [5]. However, even with the odd-parity RMF, small RMF amplitudes of $B_{rmf} < 0.07\ B_0$ are still required to keep the field-lines closed. Most present RMF-FRC experiments operate with large amplitudes $B_{rmf} \sim 0.1\text{-}0.3\ B_0$, which can result in open field-lines and compromised confinement. In contrast to the most of the related theoretical work which concentrates on the electron thermal confinement, this paper considers the effects of the applied RMF on the ion orbits.

2.1. Fully-penetrated RMF

Three-dimensional test particle simulations of FRC with RMF current drive have been performed using the HYM [1,2] code to study the effects of the applied RMF field on ion confinement. Initial conditions correspond to self-consistent FRC equilibrium with FRC kinetic parameter S*=10-20 and elongation E=3. Even- and odd-parity RMF is applied using the analytical form as given by Glasser and Cohen [4]:

Even-parity	Odd-parity
$A_z = AI_1(kr)\cos(kz)\sin(\varphi-\omega t)$	$A_z = -AI_1(kr)\sin(kz)\sin(\varphi-\omega t)$
$A_R = AI_0(kr)\sin(kz)\sin(\varphi-\omega t)$	$A_R = AI_0(kr)\cos(kz)\sin(\varphi-\omega t)$
$A_\varphi = AI_0(kr)\sin(kz)\cos(\varphi-\omega t)$	$A_\varphi = AI_0(kr)\cos(kz)\cos(\varphi-\omega t);\quad k=\pi/2Z_s$

Here A_i is component of the RMF vector potential, I_0 and I_1 are modified Bessel functions, Z_s is the separatrix half-length, and ω is the RMF frequency. Due to relatively large FRC elongation, argument of the Bessel functions is small for all r ($kr < 1$), and the above analytical form corresponds to a case of fully-penetrated RMF.

Initial set of simulations has been performed for stationary RMF ($\omega_{RMF} = 0$) of relatively large amplitudes $B_{RMF} = 0.05B_{ext}$ and $0.10B_{ext}$ in order to study the effect of the RMF-related field-line opening on ion trajectories. It is found that for FRCs with relatively large ion Larmor radius (i.e. in the small-S* FRC), there is very little difference between even- and odd-parity RMF in terms of the particle losses. There is particle loss of 17% at $t\omega_{ci} = 1000$ ($t = 25t_A$) for zero RMF amplitude, which is related to the loss of initially non-confined particles from the open magnetic field lines (Alfven time scale is $t_A = 40/\omega_{ci}$). Additional losses of 4.5% and 7% particles are caused by field-line opening due to applied stationary RMF field with $B_{RMF}=0.05$ and $B_{RMF}=0.10$ respectively. In these cases the loss rate remains finite and does not show saturation at $t\omega_{ci} \geq 1000$, which corresponds to a configuration with very long (and spiraled) open magnetic field lines. Simulations show that the rate of particle losses is generally small, but it increases in the larger FRC (i.e. larger S*) and for larger RMF amplitudes.

In contrast, high-frequency ($\omega_{RMF} >> \omega_{ci}$) RMF can have significant effect on ion losses due to ponderomotive forces (Figs. 1 and 2). In case of even-parity RMF the ponderomotive potential is antisymmetric relative to the FRC midplane: $V=\omega_p^2/(16\pi\omega^2)|E|^2 \sim \sin^2(kz)$ and it forms a potential well at z=0, whereas for the odd-parity RMF the ponderomotive potential is symmetric $V\sim\cos^2(kz)$, corresponding to a

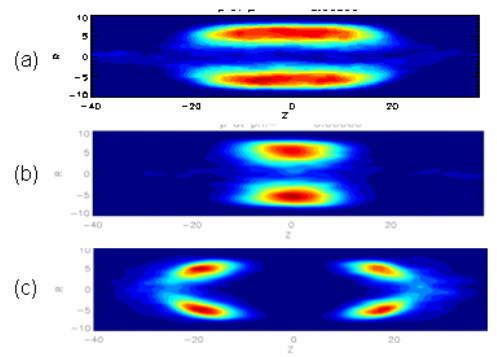

FIG. 1. *Contour plots of ion density obtained from 3D test particle simulations of FRC with applied RMF; (a) initial density contours, (b) for even parity RMF and (c) for odd parity at* $t\omega_{ci}$ *=100;* B_{RMF}*=0.10 and* ω_{RMF}*= 10*ω_{ci}.

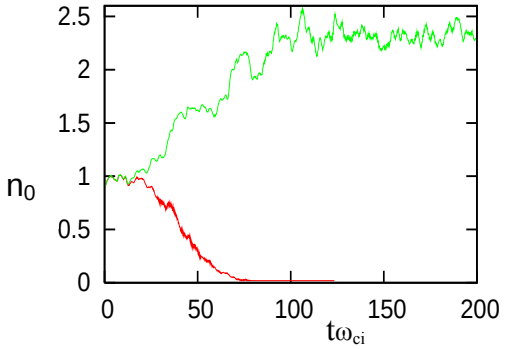

FIG. 2. *Time evolution of the normalized ion density at the FRC midplane for even parity RMF (green) and odd parity (red) for* B_{RMF}*=0.10 and* ω_{RMF}*= 10*ω_{ci}.

potential hill at z=0. As a result, high-frequency, even-parity RMF forces plasma toward the FRC midplane (Fig. 1b), but the odd-parity RMFs forces ions away from the midplane toward the FRC ends (fig. 1c). The initial and resulting ion density contours for even- and odd-parity RMF are shown in Fig. 1. Figure 2 shows time evolution of the normalized ion density at the configuration midplane (radial location of the magnetic null point at t=0). In the case of odd-parity RMF, the ion density drops to zero in about 10 ion cyclotron periods, whereas application of the even-parity RMF increases the midplane ion density by a factor of two due to axial contraction of the plasma. Calculations also show that for typical experimental parameters, the effective ponderomotive potential is significantly higher than the initial electron temperature, i.e. V~200eV.

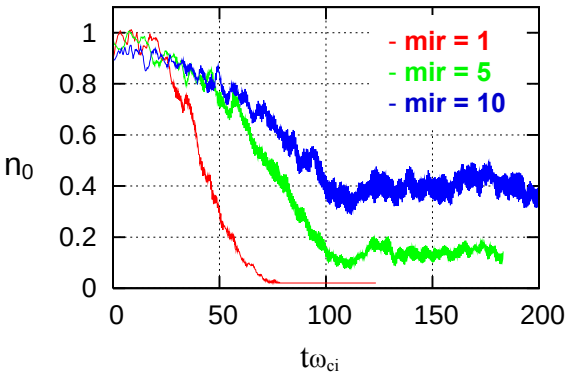

FIG. 3. *Time evolution of the normalized ion density at the FRC midplane from simulations with odd-parity RMF with different mirror ratio;* B_{RMF}*=0.10 and* ω_{RMF}*= 10*ω_{ci}.

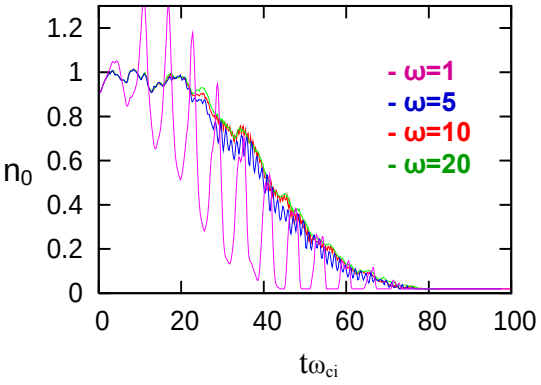

FIG. 4. *Time evolution of the normalized ion density at the FRC midplane from simulations with odd-parity RMF and different RMF frequencies* ω_{RMF}*= 1,5, 10, 20*ω_{ci}.

Additional simulations have been performed to study the effects of large mirror ratio and different RMF frequencies on ion orbits for the odd-parity RMF. Figure 3 shows time evolution of the midplane ion density for different mirror ratio. Large mirror ratio slows down the ion density decrease and the FRC break up, because magnetic mirror forces near the FRC ends are opposite to the RMF ponderomotive forces. In case of mirror ratio

of 10 and the RMF amplitude $B_{RMF}=0.1B_0$, the midplane plasma density remains finite, and the ion density contours show the elongated structure rather than two separated plasma rings. This can explain the results of the Princeton FRC experiment, where large mirror ratio is required to obtain good plasma with the odd-parity RMF current drive.

Effects of the variation of the RMF frequency are shown in Fig. 4. For sufficiently large frequencies $\omega_{RMF}\geq 5\omega_{ci}$, there are no significant differences in the ion behavior. This is expected, because for given RMF amplitude, the ponderomotive potential is independent on the RMF frequency. However, when the RMF frequency is comparable to the ion cyclotron frequency, significant ion density oscillations are observed at the midplane (Fig.4), and most of the ions are lost in a very short time $t\omega_{ci}\sim 100$.

2.1. Partially-penetrated RMF

Effects of partially penetrated RMF field on ion confinement have been studied using model RMF description. This model assumes relatively narrow penetration depth $\delta=0.2R_s$, and corresponding ratio of radial-to-toroidal RMF components $B_r/B_\varphi\sim\delta/R_s$ [6]. Other RMF and FRC parameters are $x_s=0.8$, mirror ratio = 1.5, $B_{RMF}=0.1$, and $\omega_{RMF}=10\omega_{ci}$. Figure 5a shows vector plot of the model RMF field at the FRC midplane. Three-dimensional test particle simulations have been performed for both even- and odd-parity RMF symmetry. The simulation results show that difference between even and odd-parity RMF confinement is small, provided that $\delta<<R_s$. In this case, the ponderomotive forces are edge-localized and directed radially inward, improving the particle confinement for both even- and odd-parity. Figure 5b shows poloidal contour plots of the initial ion density and the ion density at time $t\omega_{ci}=250$ for odd-parity RMF, showing very little change in the density profiles compared to the cases of fully penetrated RMF in Fig.1.

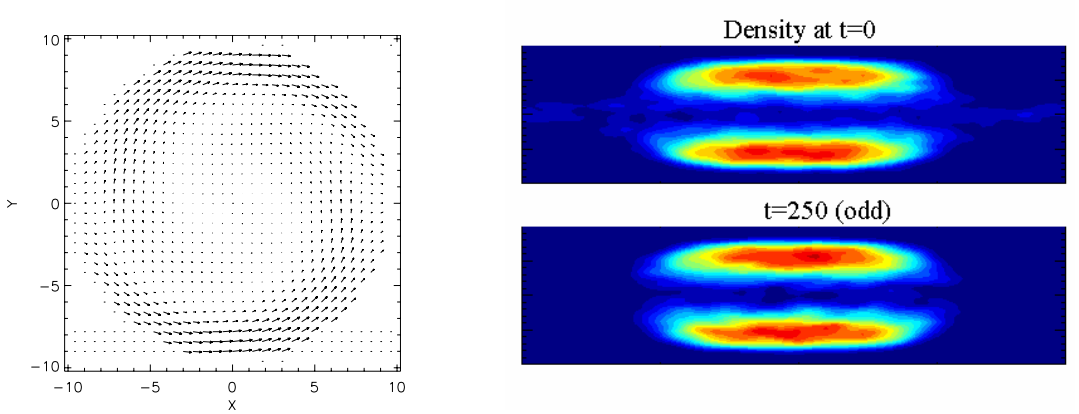

FIG. 5. *(a) Vector plot of the partially penetrated RMF field at the FRC midplane; (b) Poloidal contours of initial and final ion density from simulations for odd-parity RMF with $B_{RMF}=0.1$, mirror ratio=1.5, and $\omega_{RMF}=10\omega_{ci}$.*

3. Self-consistent Simulations

The HYM code has been modified to include the effects of rotating magnetic field (RMF) current drive for self-consistent 3D hybrid simulations. Initial plasma profiles for these simulations are shown in Fig.6. Simulations with finite open-field-line density show that the RMF pushes the plasma radially inward, resulting in a reduced plasma density outside the separatrix. A minimum (floor) value of plasma density n_c has been imposed in the simulations in order to satisfy the Courant condition for a fixed simulation time step. Simulations with large n_c and small RMF amplitude show that the RMF can penetrate only into a narrow layer near the simulation boundary, and its amplitude is significantly amplified in this region [Figs. 7a and 7b]. In contrast, lower n_c values and larger B_{RMF} values result in a deeper and faster RMF field penetration inside the plasma (Fig.8), which drives electron current in the plasma edge.

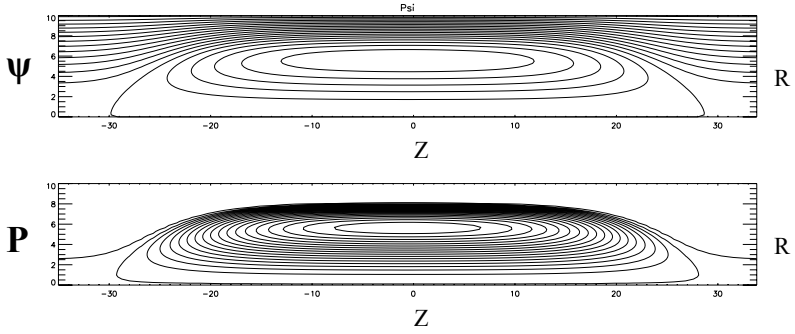

FIG 6. Initial contour plots of poloidal flux and plasma pressure for 3D self-consistent hybrid simulations of RMF current drive; E=4.5, S=4.*

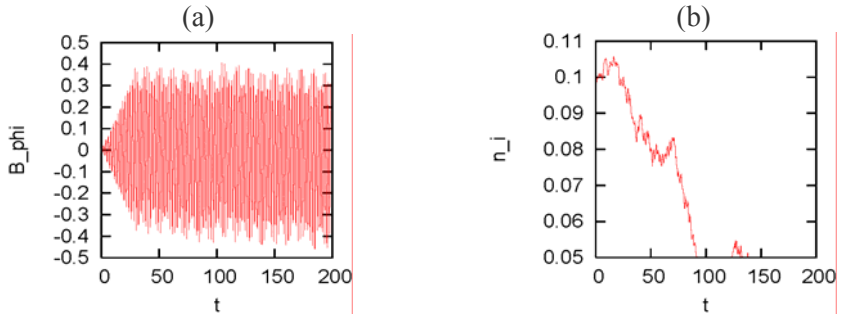

FIG 7**.** *Time evolution of the toroidal magnetic field (a) and ion density (b) near the plasma edge obtained from 3D hybrid simulations of RMF current drive with floor density n_c=0.05 and B_{RMF}=0.03. The RMF frequency is ω_{RMF}= 3ω_{ci}.*

Since finite plasma density on open field lines slows down RMF penetration and the RMF current drive, while finite resistivity causes plasma diffusion across the separatrix, thus increasing plasma density on the open field lines, the RMF applied to existing FRC have to penetrate inside plasma faster than resistive flux loss to be able to sustain current. A competition between resistive diffusion and rate of RMF penetration may explain the

relative difficulty of using RMF to drive current in the pre-formed FRC, compared to formation of an FRC using the RMF.

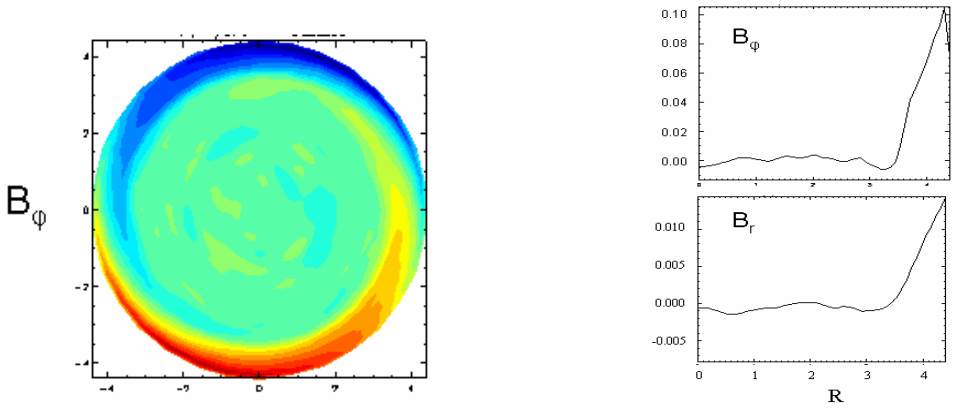

FIG. 8**.** *(a) Contour plot of the partially penetrated RMF field at the FRC midplane; (b) Radial profiles of toroidal and radial components of RMF field at the midplane obtained from simulations with beta$_s$=0.03, E=4., x_s=0.8 for even-parity RMF with B_{RMF}=0.1, and ω_{RMF}=2ω_{ci}.*

Figure 8a show contour plot of toroidal component of RMF at the FRC midplane from self-consistent 3D hybrid simulations for B_{RMF}=0.1, and ω_{RMF}=2ω_{ci}. The RMF penetration depth is approximately δ=0.1R_s, where R_s=4, and all lengths are normalized to the ion collisionless skin depth. Figure 8b shows radial profiles of toroidal and radial components of the RMF field where B_r/B_φ=0.14. Similar penetration depths and amplitude ratio are observed in the even-parity RMF experiments [6]. Self-consistent hybrid simulation consistently show generation of the axisymmetric toroidal field during the RMF penetration, which is most likely related to the nonuniform electron toroidal rotation during the initial current drive. It is found that RMF penetrates faster for configurations with low separatrix beta. It is also shown that RMF can reduce edge current (instead of driving stronger current), when initial electron rotation frequency at the edge is larger than the applied RMF frequency.

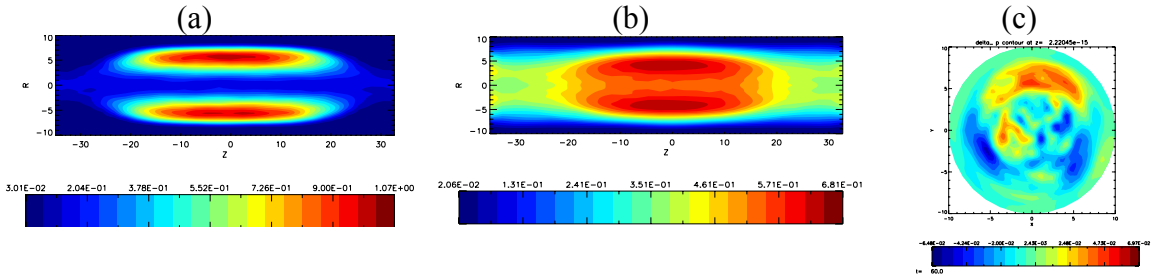

FIG.9. Density contours from 3D self-consistent hybrid simulations; (a) initial density contours in the poloidal plane; (b) change in the density contours after the RMF partially penetrated at the plasma edge; (c) contour plot of density perturbation in the midplane.

Self-consistent simulations for the even-parity RMF show that partial RMF penetration forces the FRC to contract axially (Fig. 9b), but the changes in the plasma density profiles are smaller than the test-particle simulations shown in Fig. 1b. It is also found

that low-toroidal-mode number perturbations (Fig. 9c) grow during the simulation of RMF current drive, implying that RMF does not provide complete stabilization of these modes.

Acknowledgments
The simulations reported here were carried out using resources of the National Energy Research Scientific Computing Center. This research was supported by the U.S. Department of Energy.

References
[1] BELOVA, E. V., R. C. DAVIDSON, H. JI, M. YAMADA, Phys. Plasmas **13,** 056115 (2006).
[2] BELOVA, E. V., R. C. DAVIDSON, H. JI et al., Nuclear Fusion **46,** 162 (2006).
[3] MILROY, R., Phys. Plasmas **8**, 2804 (2001); **6,** 2771 (1999).
[4] GLASSER, A. H. AND S. COHEN, Phys. Plasmas **9**, 2093 (2002).
[5] COHEN, S. A., AND MILROY, R. D., Phys. Plasmas **7**, 2539 (2000).
[6] HOFFMAN, A. L., GUO, H. Y., MILLER, K. E., MILROY, R. D., Phys. Plasmas **13**, 012507 (2006).